

Current percolation and anisotropy in polycrystalline MgB_2

M. Eisterer,^{1,*} M. Zehetmayer,¹ and H. W. Weber¹

¹ *Atominstytut der Österreichischen Universitäten, A-1020 Vienna, Austria*

(Dated: October 30, 2018)

The influence of anisotropy on the transport current in MgB_2 polycrystalline bulk samples and wires is discussed. A model for the critical current density is proposed, which is based on anisotropic London theory, grain boundary pinning and percolation theory. The calculated currents agree convincingly with experimental data and the fit parameters, especially the anisotropy, obtained from percolation theory agree with experiment or theoretical predictions.

PACS numbers: 74.70.Ad, 74.81.Bd, 64.60.Ak, 74.25.Sv

Soon after the discovery of superconductivity in MgB_2 [1], it was found that grain boundaries do not limit the current flow in polycrystalline samples [2, 3]. Thus, sintered bulk samples and wires could be prepared with critical current densities appropriate for technical applications at low magnetic fields [4]. With increasing field the critical current rapidly decreases, becoming zero at a field far below the upper critical field. Anisotropy, observed on thin films [5] for the first time, was identified as a possible reason for this strong field dependence [6]. The aim of this letter is to evaluate the influence of anisotropy on the field dependence of J_c in terms of percolation theory [7, 8]. Percolation theory had been employed frequently to analyze currents in granular superconductors [9, 10, 11, 12, 13, 14, 15, 16, 17], especially in high temperature superconductors, where grain boundaries limit the current flow, and also to interpret the irreversibility line in MgB_2 coatings [6]. We present a percolation model for the limitation of the transport current by anisotropy. While some details refer to MgB_2 , the model is applicable to any granular anisotropic superconductor or, more generally, to other systems with spatially inhomogeneous transport properties.

The superconductor is assumed to consist of randomly oriented grains with exactly identical properties. Thermal activation of the flux line lattice is neglected, since its influence in granular MgB_2 should not be much larger than in the low- T_c materials NbTi or Nb_3Sn [5] (this simplification might be the reason for some systematic deviations at high temperatures, cf. below). At fixed temperature the upper critical field only depends on the angle between the boron layers in the grain and the applied magnetic field according to the anisotropic Ginzburg Landau relation [18]

$$B_{c2}(\theta) = \frac{B_{c2}(\pi/2)}{\sqrt{\gamma^2 \cos^2(\theta) + \sin^2(\theta)}} \quad (1)$$

γ denotes the anisotropy factor of the upper critical field, i.e. $B_{c2}(\pi/2)/B_{c2}(0) =: B_{c2}^{\parallel}/B_{c2}^{\perp}$, and θ is the angle between the applied field and the c-axis. This relation was confirmed experimentally in MgB_2 by torque measurements [19, 20]. We start by considering the resistive

transition in decreasing temperature at fixed field B_0 . At a certain temperature, B_{c2}^{\parallel} becomes equal to the applied field B_0 and the resistivity starts to decrease. This point is per definition B_{c2} of the whole sample. When the temperature decreases further, an increasing number of grains becomes superconducting, depending on their orientation. During this transition the system can be considered as a mixture of normal and superconducting grains. Systems consisting of two materials with different resistances (conducting/insulating [21, 22, 23, 24] or normal/superconducting [25, 26]) have been investigated experimentally and are well understood in the framework of percolation theory. In mixtures of normal and superconducting powders the resistivity remains finite as long as the probability p , that a grain is superconducting (i.e. the fraction of superconducting grains), is smaller than the critical probability or percolation threshold p_c . The percolation threshold strongly depends on the number of connections to neighboring grains and, therefore, on the preparation conditions. When the fraction of superconducting particles becomes equal to the critical probability, the first continuous superconducting current path occurs and the resistivity disappears for sufficiently small currents. Since the upper critical field increases monotonically with θ , an angle θ_c corresponds to the critical probability within the transition region. If the boron planes are randomly oriented, the directions of the c-axes are equally distributed in 3D space and their angles to any fixed direction are distributed as $\sin(\theta)$. Integration leads to $\theta_c = \arccos(p_c)$. With $B_{c2}(\pi/2) = B_0$ and $B_{c2}(\theta_c) = B_0$ for the onset and the offset of the transition, and assuming $\frac{\partial B_{c2}}{\partial T}$ and γ to be constant within the transition region, the transition width is obtained from (1):

$$\Delta T_a = \frac{\sqrt{(\gamma^2 - 1)p_c^2 + 1} - 1}{(-\frac{\partial B_{c2}}{\partial T})} B_0 =: \frac{f_{tw}(\gamma, p_c)}{(-\frac{\partial B_{c2}}{\partial T})} B_0 \quad (2)$$

ΔT_a represents the broadening of the transition only due to the anisotropy and is, therefore, additive to other reasons for a finite transition width, e.g. material inhomogeneities, thermal fluctuations, thermal gradients in the sample, surface effects etc. The numerator of (2), f_{tw} ,

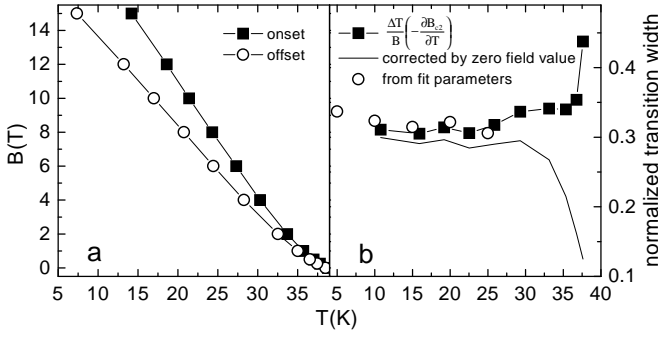


FIG. 1: Onset and offset (a) of the resistive transition in bulk MgB_2 and normalized transition width (b).

can be expressed explicitly and interpreted as a normalized transition width. It is a monotonically increasing function of γ and p_c .

The resistive transition of a sintered bulk sample [3] was measured at fixed magnetic field at a current density of 2 kA/m^2 . The onset of the transition was defined at 95 % of the normal state resistance, the offset at 5 %. The results are plotted in Fig. 1a. From the difference of onset and offset temperature, f_{tw} is calculated and plotted in Fig. 1b (black squares) as a function of the mean value of these two temperatures. Since the contribution of anisotropy tends to zero at zero field, it cannot be dominant at low fields, which explains the upturn of the normalized transition width at high temperatures. As a simple correction, we subtract the zero field transition width (0.25 K) at all fields, which leads to the solid line (without symbols) in Fig. 1b. The upturn of the original data is removed and f_{tw} becomes nearly temperature independent below 30 K, but decreases rapidly at higher temperatures. The only temperature dependent factor in f_{tw} is the anisotropy and, indeed, a rapid decrease of anisotropy near T_c was found [20, 27]. However, the assumption that all other influences on the transition width are temperature and field independent, are not appropriate to draw exact conclusions on the temperature dependence of the anisotropy. Nevertheless, the increasing difference between the onset (B_{c2}) and the offset (irreversibility field) of the resistive transition with increasing magnetic field can be explained by anisotropy and only minor corrections are needed to obtain the field dependence of the transition width observed in experiments.

In order to derive a model for the critical currents in polycrystalline samples, grain boundaries are assumed to be the dominant pinning centers. The dependence of the critical current density on the applied magnetic field ($J_c \perp B$) is, therefore, expected to be [28]

$$J_c \propto \frac{B_{c2}^{3/2}(\theta)(1 - B/B_{c2}(\theta))^2}{\kappa^2(\theta)\sqrt{B}} \propto \frac{(1 - B/B_{c2}(\theta))^2}{\sqrt{B_{c2}(\theta)B}} \quad (3)$$

for $B \leq B_{c2}(\theta)$ and zero otherwise. This equation was originally developed for isotropic superconductors, but

anisotropy can be introduced through the angular dependence of the reversible parameters. $\kappa = \kappa_1 = B_{c2}/\sqrt{2}B_c$ was used. For the sake of simplicity, we neglect any influence of the quality of a specific grain boundary, the details of grain boundary pinning as well as the angle between the local current and the applied field, which may differ due to percolation. The main feature we wish to address, is the disappearance of the critical current as $(1 - B/B_{c2}(\theta))^2$ at high fields and its rapid decrease as $B^{-0.5}$ at low fields. With these critical current densities of individual grains, we employ results on random resistor networks to derive the critical current density of the whole sample. There, the current in a network consisting of equal resistors with a current voltage law $U \propto I^\alpha$ is given near the percolation threshold by $I = \sigma_{eff}U^{1/\alpha}$, with the conductivity $\sigma_{eff} \propto (p - p_c)^t$ [29] and $t = (d - 1)\nu + (\zeta - \nu)/\alpha$ [30], where d denotes the dimensionality of the system, ζ is about one and the correlation exponent ν is 0.88 in 3D systems [31]. Most experimental data were obtained on systems consisting of normal conducting ($\alpha = 1$) and insulating particles [8, 22, 23, 24]. In this case, the above power law for σ_{eff} was found to be an excellent approximation and t to be in reasonable agreement with the theoretical prediction ($t = 1.88$). The above dependence of t on α was confirmed numerically for 2D nonlinear resistor networks [29]. Its asymptotic ($\alpha \rightarrow \infty$) value, $t = (d - 1)\nu$, was proven for all dimensions [32] ($t = 1.76$ for $d = 3$). In the following we assume α to be infinite and t to be 1.76, which makes the current independent of the voltage ("hard" superconductor), but the argument remains essentially the same for any other α at fixed voltage. Note that the influence of α on t is very weak in 3D systems. In a granular superconductor the conductivity σ_{eff} becomes a function of the (local) current density J , if p is interpreted as the fraction of grains with critical current densities larger than J . With the sample cross section σ_0 and with an appropriate normalization to get correct results for $p = 1$, the conductivity (current) becomes $I = \sigma_{eff} = \sigma_0 \left(\frac{p(J) - p_c}{1 - p_c} \right)^t J =: \sigma_p J$. We introduce σ_p , which can be interpreted as the total cross section of all current paths existing at a certain fraction p of conducting particles. If the current is smaller than $\sigma_0 \min_\theta (J_c(B, \theta))$, p is one and the current flows homogeneously through the whole superconductor. Upon enhancing the current by ΔI , p becomes smaller than one and the current density in the remaining current paths increases by $\Delta J = \Delta I / \sigma_p$. The remaining capability of the grains to carry additional currents is reduced by ΔJ . The current can be further enhanced until $p = p_c$. Integrating over all infinitesimal small ΔI (or more easily ΔJ) and division through σ_0 leads to the macroscopic

critical current density of the sample:

$$J_c(B) = \int_0^{J_c^{max}(B)} \left(\frac{p(J) - p_c}{1 - p_c} \right)^t dJ \quad (4)$$

where $J_c^{max}(B)$ is defined by $p(J_c^{max}(B)) = p_c$. In order to evaluate this expression numerically, 1001 grains were chosen with $\sin(\theta)$ equally distributed between 0 and 1. Their critical currents were calculated according to (3) and the probability distribution p was calculated basically by counting the number of grains with a critical current density above a certain value. The integral was then replaced by a summation over the discrete critical current densities of the chosen grains. The model contains four parameters: the upper critical field B_{c2} , the absolute value of the critical current densities in (3), the critical probability p_c , and the anisotropy γ . While B_{c2} can be measured directly at high temperatures and extrapolated to low temperatures, the remaining parameters are obtained by fitting the logarithm of $J_c(B)$ obtained from (4) to the corresponding experimental data with the least squares method. Two samples were used to compare experimental results with the predictions of the model, a sintered bulk sample and a Cu-sheathed powder-in-tube wire, prepared by an in-situ process [33]. The samples were neutron irradiated in a fission reactor, in order to change the reversible properties. Details of the irradiation experiments can be found in [34, 35]. The upper critical field of a similar bulk sample (from the same pellet) was determined by the onset of the resistive transition (Fig. 1a) and the linear behavior below 30 K was extrapolated to lower temperatures. For the wire, the onset of the resistive transition cannot be evaluated for B_{c2} due to the low resistance of the copper sheath. Therefore, B_{c2} was obtained from SQUID measurements. The critical current densities of the bulk sample were obtained from ac susceptibility measurements, at high critical current densities by a technique described in [36], and near the irreversibility line by evaluating the magnitude of the out-of-phase component in terms of the Bean model. Since the first method is only applicable, if the ac penetration depth is much smaller than the sample radius, and the latter, if it is larger, intermediate current densities were not evaluated. In the case of the wire, direct transport measurements were made in liquid helium.

The results are plotted in Fig. 2a together with the fitted curves (solid lines). Since the excellent agreement between experimental and calculated data (obtained by a three parameter fit) might not be unique to the proposed model, it is most important that the fit parameters (Table I) are indeed in agreement with expectations. The anisotropy is found to be 4.4 for both unirradiated samples. Literature data range from slightly above 1 to 9 [4] and are obviously sample dependent. A direct determination of the B_{c2} anisotropy was made on single crystals

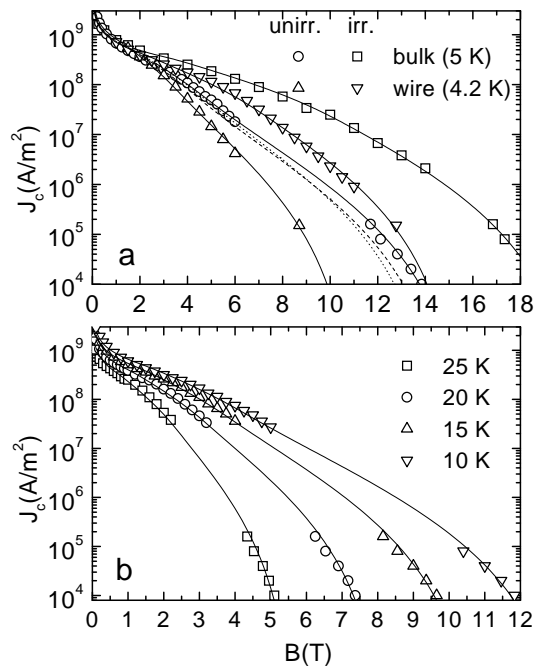


FIG. 2: Critical current densities of various samples at low temperatures (a) and of bulk MgB₂ at higher temperatures (b). The solid lines represent the fit.

($\gamma = 4.6$ [20]), aligned powders ($\gamma = 1.7$ [37]) and thin films ($\gamma = 1.2 - 2$ [5]). For sintered polycrystalline samples (wires, bulk), the anisotropy was extracted by a special technique from magnetization measurements and estimated to be 6–7 [38]. The large differences indicate that disorder affects anisotropy. This is directly confirmed here by radiation-induced disorder (Table I). The percolation threshold p_c is similar in the unirradiated samples (0.21 and 0.26). Theoretical predictions for site percolation are about 0.2 for the face centered cubic lattice (coordination number $Z=12$) and 0.31 for the simple cubic lattice ($Z=6$) [39]. Although the grains in our samples are not arranged in a regular lattice, our result indicates that on average each grain is connected to 6–12 neighboring grains. This has been confirmed by SEM investigations. Other experimental data range from 0.17 in pressed mixtures of conducting spheres and Teflon powder [24], to 0.31 in systems consisting of silver coated and uncoated glass beads [22] or 0.47 in granular W-Al₂O₃ films [23].

Experimental data on the unirradiated bulk sample at higher temperatures and the fitted $J_c(B)$ curves are plotted in Fig. 2b, the resulting values of γ and p_c in Fig. 3. While a temperature dependence of the B_{c2} anisotropy was also found in single crystals [19, 20] and powders of MgB₂ [27], the increase of p_c with increasing temperature is quite unexpected, since p_c should only depend on the arrangement of the grains within the sample. In order to explain this temperature dependence, we investigate the influence of γ and p_c on the critical currents. The dotted line in Fig. 2a represents the calculated current densi-

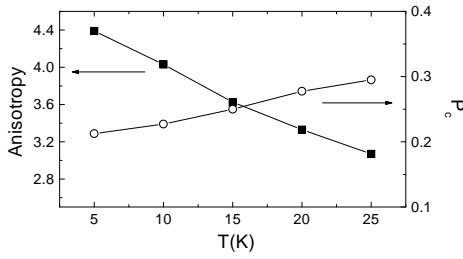


FIG. 3: Temperature dependence of the anisotropy and of the percolation threshold in bulk MgB₂.

ties, if p_c of the unirradiated bulk sample is enhanced by 20 %, leaving the other parameters constant. This has very little effect for fields below B_{c2}^\perp . An increase of the anisotropy by only 10 % (dashed line in Fig. 2a) significantly decreases the critical currents to much lower fields. The very small influence of p_c compared to γ at low fields makes the evaluation of the anisotropy quite robust against changes in p_c . On the other hand, at a given anisotropy, p_c determines the irreversibility field and, therefore, the transition width. The fit parameter p_c cannot be interpreted only as the percolation threshold anymore, because it also contains any other broadening effects on the transition. Especially thermal fluctuations lead to an artificial increase of the percolation threshold at high temperatures, but also material inhomogeneities enhance p_c . The latter explains the increase of p_c after irradiation (Table I) due to the large inhomogeneity of the defect structure following neutron irradiation [34], which leads to a significant broadening of the transition even at zero field (ΔT_c). The wire was irradiated in a cadmium cover [35], which reduces the inhomogeneity of the resulting defect structure and the enhancement of p_c .

Finally, the normalized transition width f_{tw} was calculated from the fit parameters of the unirradiated bulk sample (Fig. 1b: open circles) according to (2). The agreement with the data directly calculated from the measured transition width is very satisfactory. We conclude that the width of the resistive transition can be quantitatively explained under realistic assumptions for the anisotropy (3.1–4.4) and for the percolation probability (0.21–0.29), and that this contribution is dominant at low temperatures.

In summary, we have shown that the dependence of the critical currents in polycrystalline MgB₂ on the applied magnetic field and the broadening of the resistive transition with increasing magnetic fields can be explained by anisotropy and current percolation. The rather low upper critical field B_{c2}^\perp , turns out to be responsible for the strong field dependence of the critical current densities in polycrystalline MgB₂.

TABLE I: Experimental data on the upper critical fields (B_{c2}^\parallel) as well as anisotropy and percolation threshold obtained from the fits of the critical current densities.

	bulk (5 K)	bulk irr.	wire (4.2 K)	wire irr.
B_{c2}^\parallel (extrapol.)	21.4 T	30 T	15.4 T	18.6 T
anisotropy	4.4	2.8	4.4	2.5
B_{c2}^\perp ($:= B_{c2}^\parallel/\gamma$)	4.9 T	10.7 T	3.5 T	7.4 T
p_c	0.21	0.4	0.26	0.29

* Electronic address: eisterer@ati.ac.at

- [1] J. Nagamatsu et al., Nature (London) **410**, 63 (2001).
- [2] D. C. Larbalestier et al., Nature (London) **410**, 186 (2001).
- [3] M. Kambara et al., Supercond. Sci. Technol. **14**, L5 (2001).
- [4] C. Buzea et al., Supercond. Sci. Technol. **14**, R115 (2001).
- [5] S. Patnaik et al., Supercond. Sci. Technol. **14**, 315 (2001).
- [6] D. K. Christen et al., Mat. Res. Soc. Symp. Proc. **689**, E2.1 (2002).
- [7] D. Stauffer and A. Aharony, Introduction to Percolation Theory (Taylor & Francis, London, 1992).
- [8] S. Kirkpatrick, Rev. Mod. Phys. **45**, 574 (1973).
- [9] A. Davidson and M. Tinkham, Phys. Rev. B **13**, 3261 (1976).
- [10] G. Deutscher et al., Phys. Rev. B **21**, 5041 (1980).
- [11] O. Entin-Wohlman et al., Phys. Rev. B **30**, 2617 (1984).
- [12] E. D. Specht et al., Phys. Rev. B **53**, 3585 (1996).
- [13] M. Prester, Phys. Rev. B **54**, 606 (1996).
- [14] K. Osamura et al., Physica C **335**, 65 (2000).
- [15] R. Haslinger and R. Joynt, Phys. Rev. B **61**, 4206 (2000).
- [16] Y. Nakamura et al., Physica C **371**, 275 (2002).
- [17] B. Zeimetz et al., Eur. Phys. J. B **29**, 359 (2002).
- [18] D. R. Tilley, Proc. Phys. Soc. (London) **86**, 289 (1965).
- [19] M. Angst et al., Phys. Rev. Lett. **88**, 167004 (2002).
- [20] M. Zehetmayer et al., Phys. Rev. B **66**, 052505 (2002).
- [21] B. J. Last and D.J. Thouless, Phys. Rev. Lett. **27**, 1719 (1971).
- [22] B. Abeles et al., Phys. Rev. Lett. **35**, 247 (1975).
- [23] J. P. Clerc et al., Phys. Rev. B **22**, 2489 (1980).
- [24] S. Lee et al., Phys. Rev. B **34**, 6719 (1986).
- [25] H. J. Herrmann et al., Phys. Rev. B **30**, 4080 (1984).
- [26] G. Xiao et al., Phys. Rev. B **38**, 776 (1988).
- [27] S. L. Bud'ko and P.C. Canfield, Phys. Rev. B **65**, 212501 (2002).
- [28] D. Dew-Hughes, Phil. Mag. **30**, 293 (1974).
- [29] J. P. Straley and S. W. Kenkel, Phys. Rev. B **29**, 6299 (1984).
- [30] A. S. Skal and B. I. Shklovskii, Fiz. Tekh. Poluprovodn. **8**, 1586 (1974) [Sov. Phys. Semicond. **8**, 1029 (1975)]; P. G. de Gennes, J. Phys. (Paris) Lett. **37**, L1 (1976).
- [31] D. S. Gaunt and M. F. Sykes, J. Phys. A **16**, 783 (1983).
- [32] G. Deutscher et al., Percolation Structures and Processes (Hilger, Bristol, 1983).
- [33] B. A. Glowacki et al., Supercond. Sci. Technol. **14**, 193 (2001).
- [34] M. Eisterer et al., Supercond. Sci. Technol. **15**, L9 (2002).
- [35] M. Eisterer et al., Supercond. Sci. Technol. **15**, 1088 (2002).

- (2002).
- [36] M. Eisterer and H.W. Weber, J. Appl. Phys. **88**, 4749 (2000).
- [37] O. F. de Lima et al., Phys. Rev. Lett. **86**, 5974 (2001).
- [38] S. L. Bud'ko et al., Phys. Rev. B **64**, 180506 (2001).
- [39] S. C. van der Marck, Phys. Rev. E **55**, 1514 (1997).